



HAL
open science

Higher-order Haar wavelet method for vibration analysis of nanobeams

J. Majak, B. Shvartsman, M. Ratas, David Bassir, M. Pohlak, K. Karjust, M. Eerme

► **To cite this version:**

J. Majak, B. Shvartsman, M. Ratas, David Bassir, M. Pohlak, et al.. Higher-order Haar wavelet method for vibration analysis of nanobeams. *Materials Today Communications*, 2020, 25, pp.101290. 10.1016/j.mtcomm.2020.101290 . hal-04551782

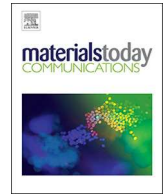
HAL Id: hal-04551782

<https://hal.science/hal-04551782>

Submitted on 6 May 2024

HAL is a multi-disciplinary open access archive for the deposit and dissemination of scientific research documents, whether they are published or not. The documents may come from teaching and research institutions in France or abroad, or from public or private research centers.

L'archive ouverte pluridisciplinaire **HAL**, est destinée au dépôt et à la diffusion de documents scientifiques de niveau recherche, publiés ou non, émanant des établissements d'enseignement et de recherche français ou étrangers, des laboratoires publics ou privés.



Higher-order Haar wavelet method for vibration analysis of nanobeams

J. Majak^{a,*}, B. Shvartsman^b, M. Ratas^a, D. Bassir^c, M. Pohlak^a, K. Karjust^a, M. Eerme^a

^a Dept. of Mech. and Industrial Eng., Tallinn University of Technology, Tallinn, Estonia

^b Estonian Entrepreneurship University of Applied Sciences, Tallinn, Estonia

^c ENS Cachan, CMLA, University of Paris Sarclay, Paris, France

ARTICLE INFO

Keywords:

Higher-order Haar wavelet method
Accuracy
Complexity
Nanobeams
Vibration

ABSTRACT

In this study, the recently developed higher-order Haar wavelet method (HOHWM) was applied in the vibration analysis of nanobeams. The method was evaluated for different boundary conditions. The complexity analysis of HOHWM was performed, and the factors influencing the complexity were determined. The numerical results obtained were compared with those of the widely used Haar wavelet method (HWM) and the exact solution. In comparison with HWM, the application of HOHWM decreased the absolute error of the solution and increased the order of convergence.

1. Introduction

The higher-order Haar wavelet method (HOHWM) was developed recently [1] as an improvement of the widely used Haar wavelet method (HWM). In the study, the HOHWM was adopted for the vibration analysis of nanobeams.

HWM was developed by Chen and Hsiao [2,3] for solving lumped and distributed parameter system problems and extended to different applications of differential [4–8], integro-differential, and integral equations [9–12]. New areas where HWM can be applied include the engineering covering analysis of composite structures [13–18] and solid mechanics [19]. In [13], HWM was applied for the free-vibration analysis of orthotropic plates. In [14], an HWM-based delamination detection algorithm was developed for composite beams. In [15,14–18], HWM was adopted for the free-vibration analysis of composite laminated conical and cylindrical shells and annular plate structures. In the monograph [19], the integration techniques used for solving differential and integro-differential equations were described, and various applications of HWM, including solid mechanics, evolution equations, optimal control theory, and damage detection using machine learning methods, were discussed. The non-uniform HVM has been described in previous studies [20,21].

Accuracy and numerical complexity are critical factors that should be considered before using any numerical method. HWM is a relatively simple method [15–19], and the convergence theorem and error estimates for HWM have been presented in [22,23]. It has been stated that the order of convergence of HWM, based on the Chen and Hsiao approach [1], is equal to two. In the case of fractional differential

equations, the convergence of HWM has been discussed in [24]. In fractional ordinary differential equations, the order of convergence of the HWM is equal to two if the higher-order derivative α in the fractional differential equation exceeds one ($\alpha > 1$) [24]. However, in the case of $0 < \alpha < 1$, the order of convergence of HWM tends to $1 + \alpha$.

Detailed comparisons of HWM, the finite difference method, and the differential quadrature method (DQM) have been drawn by a research team [22,23,25]. Based on the results obtained in [22,23,25], HWM needs to be significantly improved to compete with other efficient and straightforward formulation-based numerical methods used in engineering design, such as DQM.

Motivated by the above problem, HOHWM has been introduced in a previous study [1]. The proposed HOHWM can be used to solve complex problems with excellent accuracy. However, the HOHWM has been applied in the case of some simple problems alone. A thorough and accurate analysis is required in solving various classes of problems to obtain a more realistic picture of HOHWM. In this study, an attempt was made to use HOHWM in the vibration analysis of nanobeams.

2. Haar wavelet family

In the following analysis, the notation used in [7] is employed. The Haar functions $h_i(x)$ are defined as

$$h_i(x) = \begin{cases} 1 & \text{for } x \in [\xi_1(i), \xi_2(i)) \\ -1 & \text{for } x \in [\xi_2(i), \xi_3(i)) \\ 0 & \text{elsewhere} \end{cases} \quad (1)$$

Where

* Corresponding author.

E-mail address: juri.majak@taltech.ee (J. Majak).

$$\xi_1(i) = A + 2k\mu\Delta x, \xi_2(i) = A + (2k + 1)\mu\Delta x, \xi_3(i) = A + 2(k + 1)\mu\Delta x$$

$$\mu = M/m, \Delta x = (B - A)/(2M) \tag{2}$$

In (1) and (2), $i = m + k + 1$, where $m = 2^j$ ($M = 2^j$) corresponds to the resolution, and the parameter k indicates the location of a particular square wave. The scaling function is defined as $h_1(x) \equiv 1$; thus, $m = 0$, $\xi_1 = A$, and $\xi_2 = \xi_3 = B$. The Haar functions are orthogonal to each other and are used as basis functions. Any integrable square and finite function $f(x)$ in the interval $[A, B]$ can be expanded into Haar wavelets as

$$f(x) = \sum_{i=1}^{\infty} a_i h_i(x) \tag{3}$$

The integrals of the Haar functions (1) of order n can be computed as [7]

$$p_{n,i}(x) = \begin{cases} 0 & \text{for } x \in [A, \xi_1(i)) \\ \frac{(x - \xi_1(i))^n}{n!} & \text{for } x \in [\xi_1(i), \xi_2(i)) \\ \frac{(x - \xi_1(i))^n - 2(x - \xi_2(i))^n}{n!} & \text{for } x \in [\xi_2(i), \xi_3(i)) \\ \frac{(x - \xi_1(i))^n - 2(x - \xi_2(i))^n + (x - \xi_3(i))^n}{n!} & \text{for } x \in [\xi_3(i), B) \\ 0 & \text{for elsewhere} \end{cases} \tag{4}$$

By applying the transform $\tau = (x - A)/(B - A)$, the interval $[A, B]$ can be replaced with the unit interval $[0, 1]$.

3. HOHWM

The n -th order ordinary differential equation in the general form is considered as

$$G(x, u, u', u'', \dots, u^{(n-1)}, u^{(n)}) = 0 \tag{5}$$

Based on HOHWM introduced in [1], the Haar wavelet expansion is expressed as

$$\frac{d^{n+2s}u(x)}{dx^{n+2s}} = \sum_{i=1}^{\infty} a_i h_i(x), s = 1, 2, \dots \tag{6}$$

In (6), n represents the order of the highest derivative included in the differential equation. Hence, when $s = 1$, the derivative of order $n + 2$ is expanded into Haar wavelets. The even value of the increase in the wavelet expansion order is based on the analysis performed and previous experience.

The solution of the differential Eq. (5) $u(x)$ can be obtained by integrating (6) $n + 2$ times with respect to x as

$$u(x) = \frac{a_1 x^{n+2s}}{(n + 2s)!} + \sum_{j=0}^{\infty} \sum_{k=0}^{2^j-1} a_{2^j+k+1} p_{n+2s, 2^j+k+1}(x) + S_{BT}(x) + H_{BT}(x), \tag{7}$$

Where the boundary terms, $S_{BT}(x)$ and $H_{BT}(x)$, are expressed as

$$S_{BT}(x) = \sum_{r=0}^{n-1} c_r \frac{x^r}{r!} \tag{8}$$

$$H_{BT}(x) = \sum_{r=n}^{n+2s-1} c_r \frac{x^r}{r!} \tag{9}$$

The boundary terms $S_{BT}(x)$ and $H_{BT}(x)$ include $n + 2s$ integration constants c_r , from which n can be determined from the boundary conditions.

The higher-order wavelet expansion (6) does not provide high accuracy results. The accuracy of the solution significantly depends on the conditions used for determining the integration constants. The following two algorithms are proposed for determining the remaining 2s

integration constants [1]:

a) Uniform grid points

$$x_i = \frac{i}{N}, x_i = 1 - \frac{i}{N}, i = 0, \dots, s - 1 \tag{10}$$

b) Selected Chebyshev–Gauss–Lobatto grid points (nearest to the boundary from both sides)

$$x_i = \frac{1}{2} \left[1 - \cos \left(\frac{(i - 1)\pi}{(N - 1)} \right) \right], i = 1, \dots, s, i = N - s + 1, \dots, N \tag{11}$$

In the case of $s = 1$, both algorithms reduce to the same conditions,

$$DE(0) = G(0, u(0), u'(0), u''(0), \dots, u^{(n-1)}(0), u^{(n)}(0)) = 0,$$

$$DE(1) = G(1, u(1), u'(1), u''(1), \dots, u^{(n-1)}(1), u^{(n)}(1)) = 0 \tag{12}$$

Conditions (12) indicate that the differential equation should be satisfied at the boundary points (in addition to the collocation points).

4. Case study: Free-vibration analysis of nanobeams

In the following analysis, HOHWM is used for the free-vibration analysis of Euler–Bernoulli (EB) nanobeams. By applying the non-local Eringen theory in the differential form [26], the governing differential equation of the Euler–Bernoulli nanobeam can be derived as [27,28]

$$\frac{d^4W}{dX^4} + \frac{\mu\lambda^2}{L^2} \frac{d^2W}{dX^2} = \lambda^2 W \tag{13}$$

$$\lambda^2 = m_0 \omega^2 L^4 / EI \tag{14}$$

In (13)–(14), L denotes the nanobeam length, EI is the bending stiffness, m_0 is the moment of inertia, and ω is the natural frequency of vibration. The non-local parameter μ is defined as $\mu = e_0^2 a^2$, where e_0 and a are the material properties and internal characteristic length, respectively. The boundary conditions derived from the non-local beam theory are expressed as follows [29]:

Pinned-pinned (P-P),

$$W(0) = 0, \frac{d^2W(0)}{dX^2} + \frac{\mu\lambda^2}{L^2} W(0) = 0, W(1) = 0, \frac{d^2W(1)}{dX^2} + \frac{\mu\lambda^2}{L^2} W(1) = 0. \tag{15}$$

Clamped-pinned (C-P),

$$W(0) = 0, \frac{dW(0)}{dX} = 0, W(1) = 0, \frac{d^2W(1)}{dX^2} + \frac{\mu\lambda^2}{L^2} W(1) = 0 \tag{16}$$

Clamped-clamped (C-C),

$$W(0) = 0, \frac{dW(0)}{dX} = 0, W(1) = 0, \frac{dW(1)}{dX} = 0. \tag{17}$$

Clamped-free (C-F),

$$W(0) = 0, \frac{dW(0)}{dX} = 0, \frac{d^2W(1)}{dX^2} + \frac{\mu\lambda^2}{L^2} W(1) = 0, \frac{d^3W(1)}{dX^3} + \frac{\mu\lambda^2}{L^2} \frac{dW(1)}{dX} = 0. \tag{18}$$

The non-local boundary conditions (15)–(17) are equivalent to the corresponding boundary conditions for local beams. In the literature, condition (18) is often used in its analogue form based on the local beam theory, i.e.,

$$W(0) = 0, \frac{dW(0)}{dX} = 0, \frac{d^2W(1)}{dX^2} = 0, \frac{d^3W(1)}{dX^3} = 0. \tag{19}$$

In general, condition (18) cannot be directly reduced to (19), and such simplification is not justified if no further analysis is performed for a considered problem.

By substituting solution (7) and its derivatives into governing differential Eq. (13) and satisfying boundary conditions (15)–(18) and

Table 1
First four values of frequency parameter $\sqrt{\lambda}$ of C-C nanobeam.

N	HWM (Chen and Hsiao, 1997)				HOHWM (Majak et al., 2018)			
	$\sqrt{\lambda_1}$	$\sqrt{\lambda_2}$	$\sqrt{\lambda_3}$	$\sqrt{\lambda_4}$	$\sqrt{\lambda_1}$	$\sqrt{\lambda_2}$	$\sqrt{\lambda_3}$	$\sqrt{\lambda_4}$
4	4.2529522	5.9996954	8.2207223	8.2343050	4.2019212	5.9202688	8.1915833	8.1915833
8	4.2073252	5.8739237	7.1963937	8.2603407	4.1923145	5.8176301	7.0937118	8.1542282
16	4.1956216	5.8272627	7.1001098	8.1287993	4.1917216	5.8111156	7.0631097	8.0646311
32	4.1926692	5.8148779	7.0711262	8.0770461	4.1916850	5.8107172	7.0612321	8.0589523
64	4.1919293	5.8117403	7.0636290	8.0632499	4.1916827	5.8106925	7.0611163	8.0586046
128	4.1917442	5.8109534	7.0617398	8.0597519	4.1916825	5.8106910	7.0611092	8.0585831
256	4.1916980	5.8107565	7.0612666	8.0588744	4.1916825	5.8106909	7.0611088	8.0585817
512	4.1916864	5.8107073	7.0611482	8.0586548	4.1916825	5.8106909	7.0611088	8.0585816
Ex.	4.1916825	5.8106909	7.0611088	8.0585816	4.1916825	5.8106909	7.0611088	8.0585816

Table 2
Fundamental frequency parameters $\sqrt{\lambda_1}$, absolute errors, and rates of convergence of C-C nanobeam.

N	HWM (Chen and Hsiao, 1997)			HOHWM (Majak et al., 2018)			
	Frequency	Absolute error	Conv. rate	Frequency	Absolute error	Conv. rate	Error ratio
4	4.2529521700	6.13E-02		4.2019211501	1.02E-02		6.0
8	4.2073251614	1.56E-02	1.9697	4.1923144940	6.32E-04	4.0180	24.8
16	4.1956215705	3.94E-03	1.9896	4.1917215791	3.90E-05	4.0165	100.9
32	4.1926691558	9.87E-04	1.9973	4.1916849616	2.43E-06	4.0058	405.9
64	4.1919293050	2.47E-04	1.9993	4.1916826803	1.49E-07	4.0237	1651.3
128	4.1917442318	6.17E-05	1.9998	4.1916825402	9.35E-09	3.9991	6601.7
256	4.1916979566	1.54E-05	2.0000	4.1916825315	5.89E-10	3.9876	26180.7
512	4.1916863874	3.86E-06	2.0000	4.1916825309	4.62E-11	3.6728	83473.9
Exact	4.1916825309			4.1916825309			

Table 3
First four values of frequency parameter $\sqrt{\lambda}$ of P-P nanobeam.

N	HWM (Chen and Hsiao, 1997)				HOHWM (Majak et al., 2018)			
	$\sqrt{\lambda_1}$	$\sqrt{\lambda_2}$	$\sqrt{\lambda_3}$	$\sqrt{\lambda_4}$	$\sqrt{\lambda_1}$	$\sqrt{\lambda_2}$	$\sqrt{\lambda_3}$	$\sqrt{\lambda_4}$
4	2.8598909	4.8880373	6.3080053	6.8987493	2.8428724	4.8142654	6.3396626	7.2254732
8	2.8463962	4.8144371	6.2515130	7.4239029	2.8419048	4.7863384	6.1823723	7.3201046
16	2.8429831	4.7922526	6.1926857	7.3211362	2.8418464	4.7847254	6.1715395	7.2789698
32	2.8421278	4.7865389	6.1763981	7.2879452	2.8418427	4.7846272	6.1708930	7.2765332
64	2.8419138	4.7851009	6.1722427	7.2792892	2.8418425	4.7846211	6.1708531	7.2763842
128	2.8418603	4.7847408	6.1711988	7.2771044	2.8418425	4.7846207	6.1708506	7.2763750
256	2.8418470	4.7846507	6.1709376	7.2765569	2.8418425	4.7846207	6.1708505	7.2763744
512	2.8418436	4.7846282	6.1708722	7.2764200	2.8418425	4.7846207	6.1708505	7.2763743
Ex.	2.8418425	4.7846207	6.1708505	7.2763743	2.8418425	4.7846207	6.1708505	7.2763743

Table 4
Fourth frequency parameters $\sqrt{\lambda_4}$, absolute errors, and rates of convergence of P-P nanobeam.

N	HWM (Chen and Hsiao, 1997)			HOHWM (Majak et al., 2018)			
	Frequency	Absolute error	Conv. rate	Frequency	Absolute error	Conv. rate	Error ratio
4	6.8987493323	3.78E-01		7.2254732229	5.09E-02		7.4
8	7.4239028763	1.48E-01	1.3560	7.3201045863	4.37E-02		3.4
16	7.3211362360	4.48E-02	1.7207	7.2789698203	2.60E-03	4.0746	17.2
32	7.2879451853	1.16E-02	1.9518	7.2765332261	1.59E-04	4.0299	72.8
64	7.2792892297	2.91E-03	1.9890	7.2763842065	9.88E-06	4.0080	295.1
128	7.2771044177	7.30E-04	1.9973	7.2763749468	6.16E-07	4.0020	1184.5
256	7.2765569370	1.83E-04	1.9993	7.2763743689	3.85E-08	4.0005	4741.7
512	7.2764199873	4.57E-05	1.9998	7.2763743328	2.40E-09	4.0012	18984.5
Exact	7.2763743304			7.2763743304			

complementary conditions (12), the algebraic system of equations can be obtained to determine the values of the frequency parameter λ .

5. Numerical results and discussion

The numerical results obtained for evaluating HOHWM have high

accuracy. The results obtained by applying the widely used HWM and the HOHWM proposed by the authors are presented and compared in Tables 1–8 (grid points (10) were employed). Four different boundary conditions were examined (P-P, P-C, C-C, and C-F). The values of the non-local parameters, $\mu = 5$ and length $L = 10$ nm, were used. In Tables 1, 3, 5, and 7, the first four values of the frequency parameter for HWM

Table 5
First four values of frequency parameter $\sqrt{\lambda}$ of C-P nanobeam.

N	HWM (Chen and Hsiao, 1997)				HOHWM (Majak et al., 2018)			
	$\sqrt{\lambda_1}$	$\sqrt{\lambda_2}$	$\sqrt{\lambda_3}$	$\sqrt{\lambda_4}$	$\sqrt{\lambda_1}$	$\sqrt{\lambda_2}$	$\sqrt{\lambda_3}$	$\sqrt{\lambda_4}$
4	3.5357562	5.4539367	6.6969477	8.2279913	3.5058838	5.3700299	6.8514940	8.3621163
8	3.5108943	5.3547831	6.7237092	7.8496068	3.5026514	5.3142475	6.6376515	7.7400666
16	3.5045643	5.3220815	6.6473201	7.7305361	3.5024564	5.3108912	6.6190989	7.6780044
32	3.5029743	5.3135473	6.6254170	7.6887165	3.5024444	5.3106869	6.6179820	7.6742277
64	3.5025763	5.3113932	6.6197950	7.6776997	3.5024436	5.3106743	6.6179132	7.6739967
128	3.5024768	5.3108535	6.6183808	7.6749131	3.5024436	5.3106735	6.6179090	7.6739824
256	3.5024519	5.3107184	6.6180267	7.6742145	3.5024436	5.3106734	6.6179087	7.6739815
512	3.5024456	5.3106847	6.6179382	7.6740397	3.5024436	5.3106734	6.6179087	7.6739814
Ex.	3.5024436	5.3106734	6.6179087	7.6739814	3.5024436	5.3106734	6.6179087	7.6739814

Table 6
Second frequency parameters $\sqrt{\lambda_2}$, absolute errors, and rates of convergence of C-P nanobeam.

N	HWM (Chen and Hsiao, 1997)			HOHWM (Majak et al., 2018)			Error ratio
	Frequency	Absolute error	Conv. rate	Frequency	Absolute error	Conv. rate	
4	5.4539366655	1.43E-01		5.3700299238	5.94E-02		2.4
8	5.3547830478	4.41E-02	1.6995	5.3142475012	3.57E-03	4.0538	12.3
16	5.3220814715	1.14E-02	1.9510	5.3108911549	2.18E-04	4.0369	52.4
32	5.3135473336	2.87E-03	1.9890	5.3106869237	1.35E-05	4.0114	212.9
64	5.3113932401	7.20E-04	1.9973	5.3106742643	8.42E-07	4.0031	854.8
128	5.3108534600	1.80E-04	1.9993	5.3106734748	5.26E-08	4.0008	3422.8
256	5.3107184369	4.50E-05	1.9998	5.3106734255	3.29E-09	4.0002	13694.8
512	5.3106846762	1.13E-05	2.0000	5.3106734224	2.05E-10	4.0001	54782.8
Exact	5.3106734222			5.3106734222			

Table 7
First four values of frequency parameter $\sqrt{\lambda}$ of C-F nanobeam.

N	HWM (Chen and Hsiao, 1997)				HOHWM (Majak et al., 2018)			
	$\sqrt{\lambda_1}$	$\sqrt{\lambda_2}$	$\sqrt{\lambda_3}$	$\sqrt{\lambda_4}$	$\sqrt{\lambda_1}$	$\sqrt{\lambda_2}$	$\sqrt{\lambda_3}$	$\sqrt{\lambda_4}$
4	1.9102142	4.2167386	6.1057431	8.2168319	1.8964604	4.1031049	5.9598791	8.0646605
8	1.8998043	4.1240966	5.9401009	7.1849371	1.8963922	4.0947736	5.8620845	7.0575996
16	1.8972389	4.1016257	5.8769759	7.0712640	1.8963873	4.0942348	5.8554436	7.0290903
32	1.8965998	4.0960520	5.8605262	7.0384176	1.8963870	4.0942004	5.8550230	7.0272928
64	1.8964402	4.0946613	5.8563797	7.0299969	1.8963870	4.0941982	5.8549965	7.0271803
128	1.8964003	4.0943138	5.8553411	7.0278796	1.8963870	4.0941980	5.8549948	7.0271733
256	1.8963903	4.0942270	5.8550813	7.0273496	1.8478879	1.8963870	1.8963870	4.0941980
512	1.8963878	4.0942053	5.8550164	7.0272170	1.8963870	4.0941980	5.8549947	7.0271728
Exact	1.8963867	4.0941980	5.8549947	7.0271728	1.8963870	4.0941980	5.8549947	7.0271728

Table 8
Fundamental frequency parameters $\sqrt{\lambda_1}$, absolute errors, and rates of convergence of C-F nanobeam.

N	HWM (Chen and Hsiao, 1997)			HOHWM (Majak et al., 2018)			Error ratio
	Frequency	Absolute error	Conv. rate	Frequency	Absolute error	Conv. rate	
4	1.9102141659	1.38E-02		1.8964603982	8.55E-05		161.7
8	1.8998043116	3.42E-03	2.0166	1.8963922163	6.06E-06	3.8185	563.9
16	1.8972389104	8.52E-04	2.0040	1.8963873058	4.02E-07	3.9147	2119.3
32	1.8965997964	2.13E-04	2.0010	1.8963869780	2.59E-08	3.9583	8217.8
64	1.8964401564	5.32E-05	2.0002	1.8963869568	1.64E-09	3.9793	32439.6
128	1.8964002551	1.33E-05	2.0001	1.8963869555	1.03E-10	3.9898	129123.1
256	1.8963902803	3.32E-06	2.0000	1.8963869554	6.47E-12	3.9958	513892.4
512	1.8963877866	8.31E-07	2.0000	1.8963869554	4.09E-13	3.9841	2032319.8
Exact	1.8963869554			1.8963869554			

and HOHWM are listed. In the last row of the tables, the exact solution is presented. It can be observed from Tables 1,3,5, and 7 that the frequency values corresponding to HWM and HOHWM converge to the exact solution. However, for all the four boundary conditions considered in this study, the frequency values obtained using HOHWM were significantly more accurate than those of HWM.

In Tables 2,4,6, and 8, the values of the selected frequency, the absolute error, and the convergence rates for HWM and HOHWM are listed. It can be observed from Tables 2,4,6, and 8 that for the four considered boundary conditions, the absolute error for HOHWM is significantly smaller than that of HWM. The error ratio results presented in the last column of these tables were obtained as the ratio of

Table 9
Matrix equations for determining the values of frequency parameter λ (nanobeam, non-local theory).

Boundary conditions	HWM	HOHWM
P-P	$A_0 + A_1\lambda = 0$	$A_0 + A_1\lambda = 0$
C-P	$A_0 + A_1\lambda = 0$	$A_0 + A_1\lambda + A_2\lambda^2 = 0$
C-C	$A_0 + A_1\lambda = 0$	$A_0 + A_1\lambda + A_2\lambda^2 + A_3\lambda^3 = 0$
C-F (simplified)	$A_0 + A_1\lambda = 0$	$A_0 + A_1\lambda + A_2\lambda^2 + A_3\lambda^3 = 0$
C-F (non-local)	$A_0 + A_1\lambda + A_2\lambda^2 + A_3\lambda^3 = 0$	$A_0 + A_1\lambda + A_2\lambda^2 + A_3\lambda^3 + A_4\lambda^4 + A_5\lambda^5 = 0$

Table 10
Matrix equations for determining values of frequency parameter λ (nanobeam, non-local theory).

Boundary conditions	HWM (512 collocation points)	HOHWM (32 collocation points)	HOHWM (16 collocation points)
P-P	$512^3 \approx 1.34E+08$	$1^3 \times 32^3 \approx 3.28E+04$	$1^3 \times 16^3 \approx 4.10E+03$
C-P	$512^3 \approx 1.34E+08$	$2^3 \times 32^3 \approx 2.62E+05$	$2^3 \times 16^3 \approx 3.28E+04$
C-C	$512^3 \approx 1.34E+08$	$3^3 \times 32^3 \approx 8.85E+05$	$3^3 \times 16^3 \approx 1.11E+05$
C-F (simplified)	$512^3 \approx 1.34E+08$	$3^3 \times 32^3 \approx 8.85E+05$	$3^3 \times 16^3 \approx 1.11E+05$
C-F (non-local)	$3^3 \times 512^3 \approx 1.21E+09$	$5^3 \times 32^3 \approx 4.10E+06$	$5^3 \times 16^3 \approx 5.12E+05$

Table 11
Matrix equations for determining the values of frequency parameter λ (macro-beam, local theory).

Boundary conditions	HWM	HOHWM
P-P	$A_0 + A_1\lambda = 0$	$A_0 + A_1\lambda = 0$
C-P	$A_0 + A_1\lambda = 0$	$A_0 + A_1\lambda = 0$
C-C	$A_0 + A_1\lambda = 0$	$A_0 + A_1\lambda = 0$
C-F	$A_0 + A_1\lambda = 0$	$A_0 + A_1\lambda + A_2\lambda^2 = 0$

the errors of HWM to those of HOHWM. The rate of convergence tended to two for HWM and four for HOHWM. The formulas used for computing the rates of convergence are derived in [30].

6. Complexity analysis

The results obtained above confirm the superiority of HOHWM over HWM with respect to accuracy and convergence rate. However, extra computational costs were involved in achieving the higher accuracy, because the more accurate results were often obtained with significantly increased computational effort. In the case study, the most complex and time-consuming task involved solving the system of algebraic equations for determining the values of the frequency parameter λ . If the boundary conditions and complementary conditions are determined, the rank of the algebraic system is the same for HWM and HOHWM for the same mesh (number of collocation points). The matrix equations used for determining the values of the frequency parameter λ are expressed in Table 9. The detailed expressions of the matrices A_i are omitted in this paper for the sake of conciseness.

It can be noticed in Table 9 that the algebraic system of equations is more complex for HOHWM, except in the case of P-P boundary conditions, where the complexities of HWM and HOHWM are the same. The accuracy obtained by applying HWM at 512 collocation points was already achieved using HOHWM at 16 or 32 collocation points (Tables 2,4,6, and 8). The MATLAB function, `polyeig`, in which the generalised Schur decomposition algorithm was used to compute the eigenvalues, was applied. This approach has a cubic complexity $O(d^3N^3)$ in both the size of the matrix N and the degree d of the characteristic equation. The complexities of the solution of the algebraic systems of equations for HWM ($O(N^3)$) and HOHWM ($O(d^3N^3)$) computed for the different boundary conditions are listed in Table 10. In the case study and considered boundary conditions, the iterative solution of the 16×16 or 32×32 non-linear system (HOHWM) was computationally more straightforward than the solution of

the 512×512 linear system (HWM) system of equations.

The values of the degree d of the characteristic equation listed in Table 10 were specified based on the characteristic polynomials expressed in Table 9. The use of HOHWM produces solutions with the same accuracy and lower computation costs than HWM, despite the iterative procedure caused by the nonlinearity.

The corresponding results for macro-beams (local theory) are presented in Table 11 to understand the effect of the non-local beam theory better.

In Table 11, the C-F boundary condition was determined using (19), and the non-local conditions were omitted. In the case of the local beam theory, the characteristic equation for HOHWM was non-linear (quadratic) for only the cantilever beam. The complexity comparison of HWM results with those of HOHWM for the C-F beam was similar to that of the non-local C-P beam (see the second row of Table 10).

7. Conclusions

In this study, HOHWM was adopted for the free-vibration analysis of nanobeams. The obtained results were validated against the exact solution and compared with HWM. From the results, it was found that HOHWM outperformed HWM. The rate of convergence of HOHWM increased from two to four, and the absolute error decreased by several magnitudes (depending on selected mesh). It was shown that the numerical complexity of the solution depended on the boundary conditions and the applied local or non-local beam theory. Using selected boundary conditions, HOHWM produced results with the same accuracy at lower computational costs, in comparison with HWM. Therefore, HOHWM can be considered as an improved form of HWM.

CRedit authorship contribution statement

J. Majak: Conceptualization, Methodology, Software, Investigation, Supervision, Writing - original draft. **B. Shvartsman:** Formal analysis. **M. Ratas:** Software, Investigation. **D. Bassir:** Conceptualization, Methodology. **M. Pohlak:** Software, Writing - review & editing. **K. Karjust:** Software. **M. Eerme:** Software.

Declaration of Competing Interest

The authors declare that they have no known competing financial interests or personal relationships that could have appeared to influence the work reported in this paper.

Acknowledgments

The study was supported by the Estonian Research Council (Grant PUT1300) and the Estonian Centre of Excellence in Zero Energy and Resource Efficient Smart Buildings and Districts (ZEBE, TK146) funded by the European Regional Development Fund (grant 2014-2020.4.01.15-0016).

References

- [1] J. Majak, M. Pohlak, K. Karjust, M. Eerme, J. Kurnitski, B.S. Shvartsman, New higher order Haar wavelet method: application to FGM structures, *Compos. Struct.* 201 (2018) 72–78.
- [2] C.F. Chen, C.H. Hsiao, Haar wavelet method for solving lumped and distributed-parameter systems, *IEE Proc. Contr. Theor. Appl.* 144 (1) (1997) 87–94.
- [3] C.H. Hsiao, State analysis of the linear time delayed systems via Haar wavelets, *Math Comput. Simulat.* 44 (5) (1997) 457–470.
- [4] Ü. Lepik, Numerical solution of differential equations using Haar wavelets, *Math Comput. Simulat.* 68 (2005) 127–143.
- [5] Ü. Lepik, Haar wavelet method for nonlinear integro-differential equations, *Appl. Math. Comput.* 176 (2006) 324–333.
- [6] J. Majak, M. Pohlak, M. Eerme, T. Lepikult, Weak formulation based Haar wavelet method for solving differential equations, *Appl. Math. Comput.* 211 (2) (2009) 488–494.
- [7] Ü. Lepik, Solving PDEs with the aid of two dimensional Haar wavelets, *Comput. Math. Appl.* 61 (2011) 1873–1879.
- [8] G. Jin, X. Xie, Z. Liu, Free vibration analysis of cylindrical shells using the Haar wavelet method, *Int. J. Mech. Sci.* 77 (2013) 47–56.
- [9] S.U. Islam, I. Aziz, A.S. Al-Fhaid, An improved method based on Haar wavelets for numerical solution of nonlinear integral and integro-differential equations of first and higher orders, *J. Comput. Appl. Math.* 260 (2014) 449–469.
- [10] I. Aziz, S.U. Islam, F. Khana, A new method based on Haar wavelet for the numerical solution of two-dimensional non-linear integral equations, *J. Comput. Appl. Math.* 272 (2014) 70–80.
- [11] I. Aziz, S.U. Islam, New algorithms for the numerical solution of nonlinear Fredholm and Volterra integral equations using Haar wavelets, *J. Comput. Appl. Math.* 239 (1) (2013) 333–345.
- [12] M. Erfanian, A. Mansoori, Solving the nonlinear integro-differential equation in complex plane with rationalized Haar wavelet, *Math. Comput. Simul.* 165 (2019) 223–237.
- [13] J. Majak, M. Pohlak, M. Eerme, Application of the Haar Wavelet-based discretization technique to problems of orthotropic plates and shells, *Mech. Compos. Mater. Struct.* 45 (6) (2009) 631–642.
- [14] H. Hein, L. Feklistova, Computationally efficient delamination detection in composite beams using Haar wavelets, *Mech. Syst. Signal Pr.* 25 (6) (2011) 2257–2270.
- [15] X. Xie, G. Jin, T. Ye, Z. Liu, Free vibration analysis of functionally graded conical shells and annular plates using the Haar wavelet method, *Appl. Acoust.* 85 (2014) 130–142.
- [16] X. Xie, G. Jin, W. Li, Z. Liu, A numerical solution for vibration analysis of composite laminated conical, cylindrical shell and annular plate structures, *Compos. Struct.* 111 (2014) 20–30.
- [17] X. Xie, G. Jin, Y. Yan, S.X. Shi, Z. Liu, Free vibration analysis of composite laminated cylindrical shells using the Haar wavelet method, *Compos. Struct.* 109 (2014) 169–177.
- [18] J. Fan, J. Huang, Haar wavelet method for nonlinear vibration of functionally graded CNT-reinforced composite beams resting on nonlinear elastic foundations in thermal environment, *Shock. Vib.* 2018 (2018) 1–16, <https://doi.org/10.1155/2018/9597541>.
- [19] Ü. Lepik, H. Hein, Haar Wavelets: With Applications, Springer, New York, 2014.
- [20] Ü. Lepik, Solving integral and differential equations by the aid of non-uniform Haar wavelets, *Appl. Math. Comput.* 198 (1) (2008) 326–332.
- [21] Ö. Oruç, A non-uniform Haar wavelet method for numerically solving two-dimensional convection-dominated equations and two-dimensional near singular elliptic equations, *Comput. Math. With Appl.* 77 (7) (2019) 1799–1820.
- [22] J. Majak, B.S. Shvartsman, M. Kirs, M. Pohlak, H. Herranen, Convergence theorem for the Haar wavelet based discretization method, *Compos. Struct.* 126 (2015) 227–232.
- [23] J. Majak, B.S. Shvartsman, K. Karjust, M. Mikola, A. Haavajõe, M. Pohlak, On the accuracy of the Haar wavelet discretization method, *Compos. Part B Eng.* 80 (2015) 321–327.
- [24] J. Majak, B. Shvartsman, M. Pohlak, K. Karjust, M. Eerme, E. Tungal, Solution of fractional order differential equation by the Haar wavelet method. Numerical convergence analysis for most commonly used approach, *AIP Conf Proc* (2016) 1738, <https://doi.org/10.1063/1.4952346>.
- [25] M. Kirs, K. Karjust, I. Aziz, E. Ounapuu, E. Tungal, Free vibration analysis of a functionally graded material beam: evaluation of the Haar wavelet method, *Proc. Est. Acad. Sci.* 67 (1) (2018) 1–9.
- [26] M. Aydogdu, A general nonlocal beam theory: its application to nanobeam bending, buckling and vibration, *Physica. E* 41 (2009) 1651–1655.
- [27] M. Kirs, M. Mikola, A. Haavajõe, E. Ounapuu, B. Shvartsman, J. Majak, Haar wavelet method for vibration analysis of nanobeams, *Waves Wavelets and Fractals Advanced Analysis* 2 (2016) 20–28.
- [28] L. Behera, S. Chakraverty, Application of Differential Quadrature method in free vibration analysis of nanobeams based on various nonlocal theories, *Comput. Math. Appl.* 69 (12) (2015) 1444–1462.
- [29] P. Lu, H.P. Lee, C. Lu, P.Q. Zhang, Dynamic properties of flexural beams using a nonlocal elasticity model, *J. Appl. Phys.* 99 (2006) 073510.
- [30] B. Shvartsman, J. Majak, Numerical method for stability analysis of functionally graded beams on elastic foundation, *Appl. Math. Model.* 40 (4–5) (2016) 3713–3719, <https://doi.org/10.1016/j.apm.2015.09.060>.